Int. J. Heat Mass Transfer. Vol. 32, No. 8, pp. 1413–1423, 1989
Printed in Great Britain

0017–9310/89 $3.00+0.00

Particle rotation as a heat transfer mechanism

DAVID G. WANG, SATWINDER SINGH SADHAL and CHARLES S. CAMPBELL

Department of Mechanical Engineering, University of Southern California, Los Angeles, CA 90089-1453, U.S.A.

(*Received* 21 *March* 1988 *and in final form* 15 *November* 1988)

Abstract—A particle rotating in a temperature gradient will absorb heat from the hot side of the gradient and reject it on the cold side. This paper examines the case of a rotating solid sphere in a stationary medium on which is imposed a uniform temperature gradient. The results show that particle rotation improves the internal energy transport in much the same way as increasing the particle's thermal conductivity. At moderate values of the rotational Peclet number, the rotation induces anisotropies in the apparent thermal conductivity of the material which disappear at $Pe = 0$ and as $Pe \to \infty$.

1. INTRODUCTION

THIS WORK began as an outgrowth of an experimental project (Campbell and Wang [1]) that measured the effective conductivity of a sheared mixture of spherical particles in air. The results showed that, for fixed solid concentration, the effective conductivity of the mixture increases in direct proportion to the shear rate. The configuration of Campbell and Wang's apparatus was such that the temperature gradient and thus the direction of heat flow were in the same direction as the shear rate and perpendicular to the bulk velocity of the mixture. Thus the mean simple shear motion cannot affect the heat flow and cannot directly enhance the effective conductivity. Instead, the enhanced conductivity must result from cross-streamline energy transport accomplished by internal mechanisms that can only be indirectly related to the shear rate. Two such mechanisms were identified in that paper. The first, and the more important, can be attributed to the random motions of the individual particles which produce a turbulence-like improvement in the internal heat transport; these random velocities are induced as a byproduct of interparticle collisions, which are in turn induced by the shear rate. At the same time the shear induces particle rotation. (Reference [2] has shown that in a dry granular flow, as in nearly any shear flow, the induced rotational velocity is of the order of one-half the shear rate.) For a particle rotating in a temperature gradient, heat will be conducted into the particle on the hot side of the gradient and ejected on the cold side. Thus the rotating particle will transport heat at a rate proportional to the rotational velocity (which is, in turn, proportional to the shear rate) across a distance of the order of a particle diameter. Such a mechanism could be a most important contributor in very high density flows, where the free motion of particles is much less than a particle diameter. This paper will examine the contribution of particle rotation to the effective conductivity of the composite material.

The bulk thermal conductivity of multiphase composite materials has become a classic concern. The pioneering work is due to Maxwell [3] who, in the late 1800s, computed the effective thermal conductivity of a dilute suspension of spheres embedded in a material with a different conductivity. (Maxwell actually calculated the effective electrical conductivity, but, owing to the similarity of the equations, answered both the electrical and thermal problems simultaneously.) The effect of shear-flow-induced cross-streamline transport has been examined for dilute suspensions in the limit of low particle Reynolds numbers by Leal [4] for low Peclet numbers and by Nir and Acrivos [5] in the limit of high Peclet numbers. Both are asymptotic perturbation analyses and yield only first-order solutions. Leal showed that for small Peclet numbers, the effective conductivity grew as $Pe_f^{3/2}$. (This has been more or less confirmed experimentally by Chung and Leal [6].) Nir and Acrivos showed that at high Peclet numbers, the effective conductivity grows as $Pe_f^{1/11}$. (Here Pe_f is the fluid shear Peclet number and is equal to $R^2\gamma/\alpha_f$, where R is the particle radius, γ the shear rate and α_f the thermal diffusivity for the suspending fluid.)

However, these results are not applicable to the problem examined in ref. [1]. At low Reynolds number near the dilute limit, the particle rotation forces the neighboring fluid to rotate within a closed streamline pattern about the particle. This rotating section of fluid transports heat in much the same way as a rotating particle, and, if the heat capacity of the fluid is not negligible, much of the heat transport will take place within the fluid. In fact, at the high Peclet number limit, the depth of thermal penetration will not even extend to the particle but will be confined to a boundary layer along the outer edge of this closed streamline pattern; thus Nir and Acrivos only con-

NOMENCLATURE

a far field temperature gradient
A_1, A_2, A_3 constants defined by equations (28), (30) and (32)
A_{mn} complex constants defined by equation (19)
A_p surface area of a particle
ΣA_p combined surfaces of total particles
$B, \bar{B}$ real and imaginary part of B_{11}
B_1, B_2, B_3 constants defined by equations (29), (31) and (33)
B_{mn} complex constants defined by equation (19)
$C, \bar{C}$ real and imaginary part of C_{11}
C_{mn} complex constants defined by equation (18)
C_p specific heat of the particle at constant pressure
$E(\bar{r}), F(\bar{r})$ real and imaginary part of $\mathbf{j}_1(\mathrm{i}\sqrt{(\mathrm{Im}\ Pe)}\bar{r})$
$\mathbf{j}_n(\mathrm{i}\sqrt{(\mathrm{Im}\ Pe)}\bar{r})$ spherical Bessel functions
k thermal conductivity
K_{ij} bulk thermal conductivity, second-rank tensor
n_i unit outer normal in the i-direction
Pe particle Peclet number, $\Omega R^2/\alpha_p$
Pe_f fluid Peclet number, $\gamma R^2/\alpha_f$
$P_n^m(\cos\theta)$ Legendre's associated polynomials
q_i local conductive heat flux in the i-direction
Q_i bulk conductive heat flux in the i-direction
r radial coordinate
$\bar{r}$ dimensionless radial coordinate
R particle radius
T dimensional temperature
$\bar{T}$ dimensionless temperature
T' temperature deviation from the bulk temperature
u_i' velocity deviation in the i-direction from the mean velocity
V averaging volume
V_p volume of a particle
ΣV_p combined volumes of total particles
x, y, z coordinates, see Fig. 1.

Greek symbols
α thermal diffusivity
β dimensionless parameter, $\sqrt{(Pe/2)}$
γ fluid shear rate
η dimensionless parameter, $(k_f/k_p)\sqrt{(2/Pe)}$
θ, ϕ coordinates, see Fig. 1
ν volume fraction of particle, $\Sigma V_p/V$
ρ particle density
Ω particle rotation rate.

Subscripts
f fluid property
m, n indices
p particle property.

sidered this thin boundary layer in their analysis, and the particle appears only indirectly as the instigator of the closed streamline pattern.

Campbell and Wang's [1] experiments were performed at moderate Re and Pe, and could not be continued down into the low Re regime, as they depended on a high shear rate to keep their material in a fluidized state. Furthermore, their system was far from dilute, and, even ignoring more important effects of close particle interaction, the presence of neighboring particles may disrupt any closed streamline pattern of fluid motion and eliminate that mechanism as an important contributor to the heat transport. In fact, the fluid motion between the particles is so complex that it defies analysis, is probably due, in most part, to squeezing between colliding particles and is not induced by the particle rotation. Furthermore, if the heat capacity of the fluid is negligible (as it would be for solid particles in air), the fluid would not be a major contributor to the heat transport. Still, it is interesting to try and understand the heat transport role that particle rotation plays in such a complex environment. To this end, this analysis will examine the heat transport due to particle rotation inside a stationary medium in an attempt to decouple the rotational effects from all other heat transport mechanisms. The proposed problem is simpler than any of its predecessors and admits a complete solution for the entire range of Peclet numbers.

2. TEMPERATURE DISTRIBUTION

Consider a single rotating particle embedded in an infinite medium on which a uniform temperature gradient is imposed far from the particle. The particle is assumed to be rotating around the z-axis with angular velocity Ω, as shown in Fig. 1, while the medium surrounding the particle is stationary. In spherical coordinates, the flow field can be expressed as

$$V_\phi = \begin{cases} r\Omega \sin\theta & r \leqslant R \\ 0 & r > R \end{cases} \quad (1)$$

where R is the particle radius.

The coordinate system is chosen so that the tem-

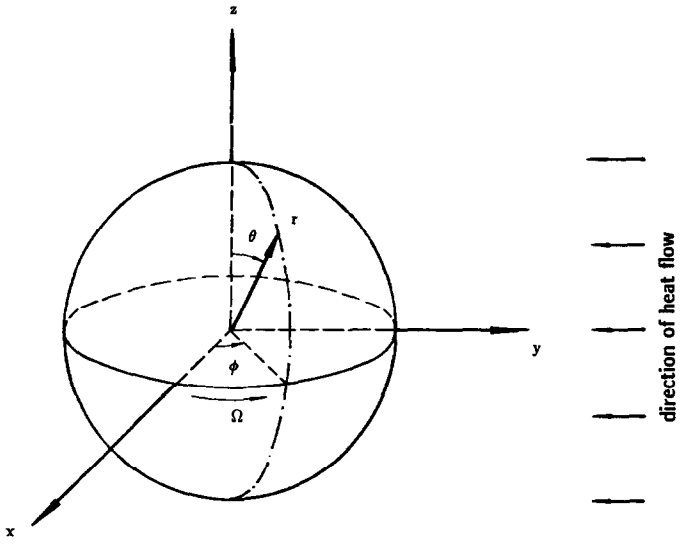

FIG. 1. Coordinate system for the rotating particle calculation.

perature gradient far from the particle is in the y-direction and approaches a uniform value of a, i.e.

$$\lim_{r\to\infty} \frac{\partial T}{\partial y} = a. \tag{2}$$

In these circumstances, the appropriate dimensional equations governing the temperature distributions inside and outside the particle are

$$\nabla^2 T_p = \frac{\Omega}{\alpha_p} \frac{\partial T_p}{\partial \phi} \tag{3}$$

$$\nabla^2 T_f = 0 \tag{4}$$

where α_p is the particle thermal diffusivity and T_p and T_f are the temperatures of the particle and the external fluid, respectively. Note that the same equations govern the heat transport in the limit that the heat capacity of the surrounding fluid is negligible compared to that of the particle so that little energy can be transported by fluid convection. (This is exactly the case in the experiments of ref. [1], for which the particles had several thousand times the heat capacity of the surrounding air.)

Equations (3) and (4) are to be solved subject to the conditions of continuity of temperature and continuity of heat flux on the particle surface, and matching the uniform temperature gradient far away from the particle

$$T_p = T_f \qquad \text{at } r = R \tag{5}$$

$$k_p \frac{\partial T_p}{\partial r} = k_f \frac{\partial T_f}{\partial r} \qquad \text{at } r = R \tag{6}$$

$$T_f \to ar(\sin\theta \sin\phi) \qquad \text{at } r \to \infty \tag{7}$$

where k_p and k_f are the conductivities of the particle and the external fluid, respectively. Owing to the symmetries of the problem about the particle center

$$T_p = 0 \quad \text{at } r = 0. \tag{8}$$

By introducing two dimensionless quantities

$$\bar{T} = \frac{T}{aR} \tag{9}$$

$$\bar{r} = \frac{r}{R} \tag{10}$$

equations (3) and (4) become

$$\nabla^2 \bar{T}_p(\bar{r}, \theta, \phi) = Pe \frac{\partial \bar{T}_p}{\partial \phi} \tag{11}$$

$$\nabla^2 \bar{T}_f(\bar{r}, \theta, \phi) = 0 \tag{12}$$

where Pe is the particle Peclet number defined as

$$Pe = \frac{\Omega R^2}{\alpha_p} \tag{13}$$

and the boundary conditions (5)–(8) become

$$\bar{T}_p = \bar{T}_f \qquad \text{at } \bar{r} = 1 \tag{14}$$

$$\frac{\partial \bar{T}_p}{\partial \bar{r}} = \frac{k_f}{k_p} \frac{\partial \bar{T}_f}{\partial \bar{r}} \qquad \text{at } \bar{r} = 1 \tag{15}$$

$$\bar{T}_f \to \bar{r} \sin\theta \sin\phi \qquad \text{at } \bar{r} \to \infty \tag{16}$$

$$\bar{T}_p = 0 \qquad \text{at } \bar{r} = 0. \tag{17}$$

In the limit $Pe \to \infty$, equation (11) implies that $\partial \bar{T}_p / \partial \phi \to 0$, or that, in this limit, the temperature about the circumference of the particle must be uniform. It is reasonable to assume that the particle surface will adopt the average temperature to which it is exposed—which, by the symmetry of the problem, is zero. This observation, coupled with the additional symmetry condition, equation (17), that the temperature at the center of the particle must be zero, leads to the conclusion that in the limit of high Peclet numbers, the particle temperature approaches a uniform temperature which must be zero. (At large but finite Peclet numbers, any temperature changes within

the particle will be confined to a thermal boundary layer about the outer edge of the particle, but even this thin boundary layer will disappear as $Pe \to \infty$.) From a purely physical standpoint, this can be understood, as, when $Pe = \infty$, any non-zero temperature inside the particle will lead to an infinite convective heat transport rate, which would then require that an infinite quantity of heat be conducted to and from the particle through the surrounding medium; such a burden cannot be borne by a finite conductivity material on which is imposed a finite temperature gradient. Curiously, this is exactly the same condition that is reached for a stationary particle in the limit $k_f/k_p \to 0$; in that case, any temperature gradient inside the particle will again lead to infinite heat transport rates which cannot be supported by conduction through the surrounding material, requiring once again that the particle temperature becomes uniform (and, by symmetry, equal to zero). Thus, large Pe is equivalent to large apparent particle thermal conductivity, and as $Pe \to \infty$, the situation must approach Maxwell's solution for a dispersion of stationary spheres with infinite conductivity. This places an upper limit on the heat transport that can be obtained by particle rotation, and one would expect very little effect if the conductivity ratio k_f/k_p is already very small. It is important to note that, despite the fact that this problem is being set up in the dilute limit, equation (11) and all of the conclusions that have just been drawn from it are valid regardless of the particle concentration. Thus particle rotation should contribute only slightly to the heat transport in the particle–air mixture ($k_f/k_p \simeq 0.01$) tested in ref. [1].

Equation (12), governing the heat conduction through the fluid, is readily solved for these boundary conditions by separation of variables. At the same time, a quick examination shows that the convective term in the particle temperature equation, equation (11), complicates the classical separation procedure. However, as the solution must be periodic in ϕ, it seems reasonable to choose the corresponding eigenfunction of the form $e^{im\phi}$. With this done, the problem is easily separated in the other two coordinates to yield

$$\bar{T}_p(\bar{r},\theta,\phi) = \sum_{n=0}^{\infty}\sum_{m=0}^{n} [C_{mn}\mathbf{j}_n(i\sqrt{(im\,Pe)}\bar{r}) \times P_n^m(\cos\theta)\,e^{im\phi}]. \quad (18)$$

Here the C_{mn} are complex coefficients, the $\mathbf{j}_n$ are spherical Bessel functions and the P_n^m are associated Legendre polynomials. This result was verified by substituting into the original equation (11).

The general solution of the dimensionless heat conduction equation (12) for the external medium can be solved by a quite straightforward procedure of separation of variables. Noting that the eigenfunction in ϕ should be of the same form as $\bar{T}_p$ in order to match the boundary conditions, the general solution for $\bar{T}_f$ takes the form

$$\bar{T}_f(\bar{r},\theta,\phi) = \sum_{n=0}^{\infty}\sum_{m=0}^{n} [A_{mn}\bar{r}^n + B_{mn}\bar{r}^{-(n+1)}] \times P_n^m(\cos\theta)\,e^{im\phi} \quad (19)$$

where A_{mn} and B_{mn} are complex constants.

Applying the boundary conditions (14)–(17) and taking the imaginary part yields

$$\bar{T}_p = \{E(\bar{r})[C\sin\phi + \bar{C}\cos\phi] + F(\bar{r})[C\cos\phi - \bar{C}\sin\phi]\}\sin\theta \quad (20)$$

$$\bar{T}_f = \bar{r}\sin\theta\sin\phi + \frac{[B\sin\phi + \bar{B}\cos\phi]}{\bar{r}^2}\sin\theta \quad (21)$$

where $C_{11} = C + i\bar{C}$, $B_{11} = B + i\bar{B}$, $A_{11} = 1$ and $A_{mn} = B_{mn} = C_{mn} = 0$ for all other m and n.

Here

$$E(\bar{r}) = \frac{-1}{Pe\,\bar{r}^2}\cos(\beta\bar{r})\sinh(\beta\bar{r}) + \frac{1}{\bar{r}\sqrt{(2Pe)}}[\cos(\beta\bar{r})\cosh(\beta\bar{r}) - \sin(\beta\bar{r})\sinh(\beta\bar{r})] \quad (22)$$

$$F(\bar{r}) = \frac{-1}{Pe\,\bar{r}^2}\sin(\beta\bar{r})\cosh(\beta\bar{r}) + \frac{1}{\bar{r}\sqrt{(2Pe)}}[\cos(\beta\bar{r})\cosh(\beta\bar{r}) + \sin(\beta\bar{r})\sinh(\beta\bar{r})] \quad (23)$$

$$B = \frac{3\eta(B_1B_3 - A_1A_3)}{A_3^2 + B_3^2} - 1 \quad (24)$$

$$\bar{B} = -\frac{3\eta(A_1B_3 + A_3B_1)}{A_3^2 + B_3^2} \quad (25)$$

$$C = -\frac{3\eta A_3}{A_3^2 + B_3^2} \quad (26)$$

$$\bar{C} = -\frac{3\eta B_3}{A_3^2 + B_3^2} \quad (27)$$

where

$$A_1 = E(1) \quad (28)$$

$$B_1 = F(1) \quad (29)$$

$$A_2 = \frac{1}{\sqrt{(2Pe)}}[2A_1 - 2B_1 + \sin(\beta)\cosh(\beta) + \cos(\beta)\sinh(\beta)] \quad (30)$$

$$B_2 = \frac{1}{\sqrt{(2Pe)}}[2A_1 + 2B_1 + \sin(\beta)\cosh(\beta) - \cos(\beta)\sinh(\beta)] \quad (31)$$

$$A_3 = A_2 + B_2 - 2\eta A_1 \quad (32)$$

$$B_3 = A_2 - B_2 + 2\eta B_1 \quad (33)$$

$$\beta = \sqrt{\left(\frac{Pe}{2}\right)} \quad (34)$$

$$\eta = \frac{k_f}{k_p}\sqrt{\left(\frac{2}{Pe}\right)}. \quad (35)$$

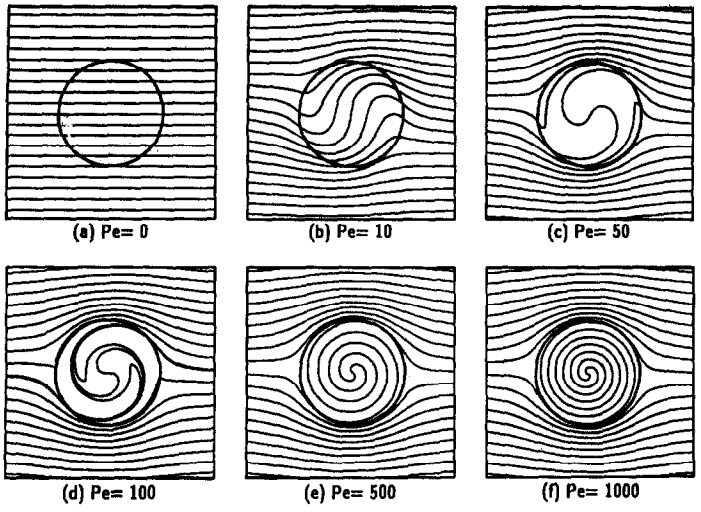

FIG. 2. The isothermal lines upon an equatorial cut through the particle for $k_f/k_p = 1.0$.

In the above, the first-order spherical Bessel function has been replaced according to the definition

$$j_1(z) = \frac{\sin(z) - z\cos(z)}{z^2}. \tag{36}$$

3. ISOTHERMS

A great deal of physical insight can be gained by examining how the particle rotation distorts the isotherms in and about the particle. Figures 2–4 show the isothermal lines on an equatorial cut on the x–y plane through the center of the particle; each is drawn so that the particles are rotating in the counterclockwise direction about an axis pointing out of the page. The figures illustrate three cases, $k_f/k_p = 1, 0.01$, and 10, as Pe is increased from 0 to 1000. Each line was found by choosing a temperature and then numerically determining the appropriate path of the isotherm corresponding to that temperature. Most of the plots start with isotherms initially spaced $\frac{1}{5}R$ apart at the far left-hand side of each frame, although, in a few cases, extra isotherms were added very near the centerline ($\bar{T} = 0$) to help fill out the pattern within the particle.

At $Pe = 0$, the $k_f/k_p = 1$ (Fig. 2(a)) isotherms are horizontal lines, while for $k_f/k_p = 0.01$ (conducting particle, Fig. 3(a)), the isotherms spread away from the particle, and for $k_f/k_p = 10$ (insulating particle, Fig. 4(a)), the isotherms converge inside the particle. Increasing the Peclet number slightly causes the isotherms external to the particle to rotate counterclockwise. As the particle itself is rotating counterclockwise, the isotherms are reacting to their memory of where the particle has been and not to where it is going. Note that at $Pe = 0$ the isotherm pattern external to the particle is symmetric about a vertical line through the center, becomes skewed for low Pe, and at high Pe again adopts a symmetric pattern. The

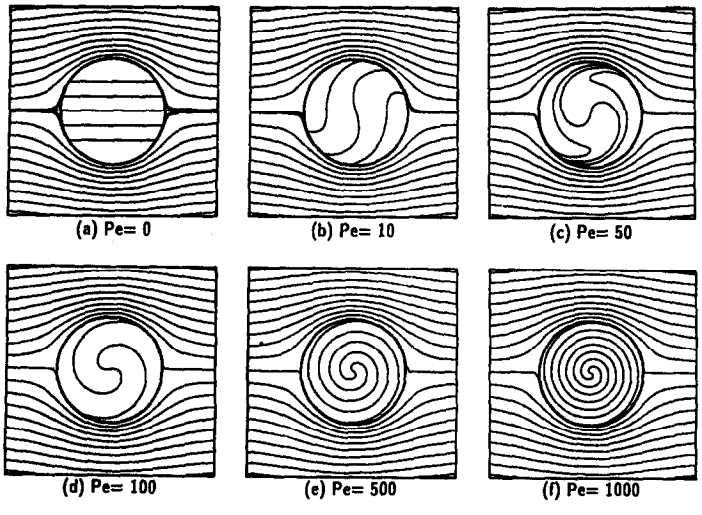

FIG. 3. The isothermal lines upon an equatorial cut through the particle for $k_f/k_p = 0.01$.

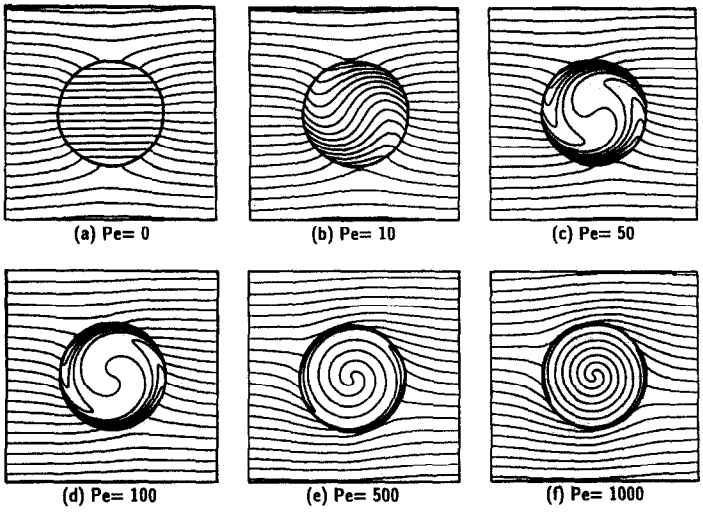

FIG. 4. The isothermal lines upon an equatorial cut through the particle for $k_f/k_p = 10.0$.

skewing of the isotherm pattern reflects temperature gradients—and hence heat flow—in the x-direction, despite the fact that the imposed temperature gradient is in the y-direction. This indicates that the rotation induces anisotropies in the apparent conductivity of the material at moderate Peclet numbers which will disappear at $Pe = 0$ and as $Pe \to \infty$.

Viewing the problem from inside the particle within a reference frame that rotates with the particle, an observer would witness alternately hot and cold temperatures traveling radially inward. This reflects the facts that the particle surface alternately experiences the hot and cold portions of the temperature gradient and that surface temperature variation appears as waves, traveling inward, with the period of the particle rotation, $1/\Omega$, and an amplitude that decreases as the center is approached. The wave travels with a speed that is related to the thermal diffusivity, α_p, and is therefore independent of the rate of rotation; hence, on purely physical grounds, one expects that the wavelength should vary with α_p/Ω and hence with the inverse Peclet number. (This suspicion is borne out by a quick examination of equation (18).) Thus one effect of changing the rotation rate is to change the wavelength of the incoming waves. At low Peclet number, the isotherms inside the particle undulate almost sinusoidally, as the wavelength is longer than the particle radius. At higher Peclet number, most of the originally internal isotherms have spread outward till they are external to the particle or within a thin thermal boundary layer at its outer edge. All that is left inside the particle is the $\bar{T} = 0$ isotherm, which, at the highest Peclet numbers, forms a double spiral heading inward towards its intersection with the center of the particle (as is required by equation (8)). The spiral of the $\bar{T} = 0$ isotherm represents the nodes in the thermal wave pattern, so that the space between them is one-half of the wavelength. By comparing Figs. 2–4, it can be seen that the spacing between the loops of the $\bar{T} = 0$ isotherm are independent of the conductivity ratio k_f/k_p, and depend only on the Peclet number, just as would be expected from the above discussion.

The formation of the thermal boundary layer at the outer edge of the particle can be observed by following the isotherms on either side of the $\bar{T} = 0$ line. At moderate to high Peclet numbers, these adopt horn-like shapes within the $\bar{T} = 0$ spiral. As the Peclet number is increased, the horn structures spread outward as the boundary layer develops. This is best observed in the $k_f/k_p = 10$ plots shown in Fig. 4, as the low conductivity particle attracts and retains the largest number of internal isotherms. For this case, the horns can still be observed for the $Pe = 1000$ case (Fig. 4(f)) at the very outer edge of the particle.

A major concern of this paper is the effect of particle rotation on the apparent conductivity. Following Fig. 2, the isotherms are horizontal for $Pe = 0$ and spread outward from the particle as the Peclet number is increased. Progressively more of the isotherms pass around and never cross into the particle, and the isotherm pattern external to the particle assumes the same symmetric pattern as that for a high conductivity non-rotating particle (such as that shown in Fig. 3(a)). This change is most extreme for the large k_f/k_p case shown in Fig. 4. There, the isotherms converge on the particle for $Pe = 0$, as is expected for insulating particles, but progressively diverge away from the particle as the Peclet number is increased. All of this is a reflection of the dimensional analysis in Section 2, which showed that increasing the Peclet number effectively increases the apparent particle conductivity. As far as the external isotherms are concerned, the particle will assume the appearance of a good conductor at high Peclet number, despite its real conductivity ratio, k_f/k_p; one consequence is that the asymmetry in the isotherms (which produces anisotropies in the bulk material conductivity), also disappears. Looking ahead to the effective material con-

ductivity derived in the next section and plotted in Fig. 5, it can be seen that the effective conductivity for the $k_f/k_p = 10$, $Pe = 500$ case plotted in Fig. 4(e) is nearly the same as that for the $k_f/k_p = 1$, $Pe = 10$ case plotted in Fig. 2(b). Moreover, comparing the two figures, it can be seen that the external isotherm patterns are identical, even though the internal patterns differ dramatically. A further consequence of the dimensional analysis argument is that rotation will not greatly affect the apparent conductivity of high conductivity particles. This can be seen in Fig. 3, as the external isotherm pattern appears unaffected by the Peclet number.

4. THE EFFECTIVE CONDUCTIVITY OF THE COMPOSITE MATERIAL

The next problem is to use the single particle calculation above to determine the effective conductivity for the particle–fluid composite. However, the observations of the last section suggest that the conductivity of the particle–fluid mixture will be anisotropic in the sense that the direction of heat flow will not necessarily coincide with the direction of the applied temperature gradient. Hence, the conductivity will be expressed as a second-rank tensor, K_{ij}, such that the bulk conductive heat flux vector, Q_i, which results from an applied temperature gradient, can be expressed as

$$Q_i = -K_{ij}\left\langle \frac{\partial T}{\partial x_j} \right\rangle \tag{37}$$

where $\langle \partial T/\partial x_i \rangle$ is an average of the temperature gradient within the material.

In general, the conductivity tensor, K_{ij}, may be found using equation (37) by imposing temperature gradients in each of the three directions and calculating the resultant Q_i and $\langle \partial T/\partial x_i \rangle$. For this particular problem, however, only two components of the conductivity tensor, K_{xy} and K_{yy}, are left to be found, and they can be determined from the single particle case, calculated in Section 2, which assumed an applied temperature gradient in the y-direction. The other seven components of K_{ij} are already known. This can be easily seen by noting that the solution is independent of rotation in the x–y plane; i.e. rotating the imposed temperature gradient about the z-axis only rotates the solution. Hence

$$K_{xx} = K_{yy} \tag{38}$$

and

$$K_{yx} = K_{xy}. \tag{39}$$

Furthermore, the particle's rotation will not aid or induce any heat transport in the axial (z) direction, so K_{zz} is given by Maxwell's [6] solution

$$\frac{K_{zz}}{k_f} = 1 + v\frac{3(1-k_f/k_p)}{2k_f/k_p + 1} \tag{40}$$

where v is the solid fraction, and

$$K_{xz} = K_{zx} = K_{yz} = K_{zy} = 0. \tag{41}$$

A great deal of controversy surrounds the proper procedure for finding macroscopic properties of a material, such as K_{ij}, from microscopic analyses like that found in Section 2. Fortunately, most of the controversy concerns multiple particle interaction and disappears in the dilute limit considered here. This paper will follow an approach similar to that used by Leal [7]. In Leal's approach, the bulk conductive heat flux for the composite material, viewed as an equivalent homogeneous medium, takes the form

$$Q_i = \langle q_i \rangle + \rho C_p \langle u_i' T' \rangle \tag{42}$$

where $\langle q_i \rangle$ is a volume average of the local conductive heat flux, u_i' the local deviation from the bulk velocity (as in this case the bulk velocity is zero, u_i' is just the rotation velocity) and T' the deviation from the undisturbed temperature field. Thus $\rho C_p \langle u_i' T' \rangle$ is the turbulence-like convective heat transport induced by the particle rotation. (Note that all of the temperatures are dimensional in this calculation.) Here, the usual notation of Cartesian tensors is employed, and the volume average of a quantity P is defined as

$$\langle P \rangle = \frac{1}{V}\int_V P \, dV \tag{43}$$

where V is a sufficiently large averaging volume containing many particles.

The average conductive heat flux is found by taking a volume average of the local heat fluxes

$$\langle q_i \rangle = -\left\langle k\frac{\partial T}{\partial x_i} \right\rangle \tag{44}$$

where k is the local thermal conductivity of the material and T the local temperature (i.e. $k = k_f$ or $k = k_p$ and $T = T_f$ or $T = T_p$, depending on whether the integrand is taken over volume elements occupied by the fluid or particle). Note that this expression may be decomposed as

$$\langle q_i \rangle = -\left\langle k_f\frac{\partial T}{\partial x_i} \right\rangle - \left\langle (k-k_f)\frac{\partial T}{\partial x_i} \right\rangle. \tag{45}$$

As k_f is assumed uniform, and $(k-k_f) = 0$, except over the volume ΣV_p, occupied by the particles (where $k-k_f = k_p-k_f$ and is constant), the second average reduces to a volume integral only over the region ΣV_p, while the first is over the entire volume V

$$\langle q_i \rangle = -k_f\left\langle \frac{\partial T}{\partial x_i} \right\rangle\Big|_V - (k_p-k_f)\left\langle \frac{\partial T_p}{\partial x_i} \right\rangle\Big|_{\Sigma V_p}. \tag{46}$$

This decomposition allows the particle and fluid solutions to be considered separately. Upon substituting equation (46) into equation (42) and applying Gauss's theorem to the volume integral over the whole volume V, the two components of the heat flux vector become

$$Q_x = -k_f\left\langle\frac{\partial T}{\partial x}\right\rangle - \frac{k_p-k_f}{V}\int_{\Sigma A_p}(n_x T_p)|_{r=R}\,dS + \frac{(\rho C_p)_p}{V}\int_{\Sigma V_p}(u_x' T_p')\,dV \quad (47)$$

and

$$Q_y = -k_f\left\langle\frac{\partial T}{\partial y}\right\rangle - \frac{k_p-k_f}{V}\int_{\Sigma A_p}(n_y T_p)|_{r=R}\,dS + \frac{(\rho C_p)_p}{V}\int_{\Sigma V_p}u_y' T_p'\,dV. \quad (48)$$

Here ΣA_p represents the combined surfaces of all the particles in V. For both cases, the first two terms represent the heat transport by conduction and the third represents the convective heat transport induced by the rotation of the particle.

Under the circumstances where the composite is infinitely dilute so that the temperature distribution about a particle is unaffected by the presence of the other particles and all the particles are of identical shape and size, the integrals over ΣA_p and ΣV_p can be taken as integrals over the single particle surface area and volume, A_p and V_p, multiplied by the total number of particles within the averaging volume of the composite. In terms of the solid fraction v, the number of particles in a volume V is given by $vV/(\frac{4}{3}\pi R^3)$. Hence, the results are at best correct to order v, and equations (47) and (48) can be rewritten as

$$Q_x = \frac{3v(k_f-k_p)}{4\pi R^3}\int_0^{\pi}\int_0^{2\pi}R^2[(n_x T_p)_{r=R}\sin\theta]\,d\theta\,d\phi + \frac{3v(\rho C_p)_p}{4\pi R^3}\int_0^{R}\int_0^{\pi}\int_0^{2\pi}[(u_x' T_p')r^2\sin\theta]\,d\phi\,d\theta\,dr \quad (49)$$

and

$$Q_y = -k_f\left\langle\frac{\partial T}{\partial y}\right\rangle + \frac{3v(k_f-k_p)}{4\pi R^3}\int_0^{\pi}\int_0^{2\pi}R^2[(n_y T_p)_{r=R}\sin\theta]\,d\theta\,d\phi + \frac{3v(\rho C_p)_p}{4\pi R^3}\int_0^{R}\int_0^{\pi}\int_0^{2\pi}[(u_y' T_p')r^2\sin\theta]\,d\phi\,d\theta\,dr. \quad (50)$$

These integrals may be calculated from the results of Section 2 by replacing T with $aR\bar{T}$ and r with $\bar{r}R$. Note that, for this particular problem

$$n_x = \sin\theta\cos\phi \quad (51)$$

$$n_y = \sin\theta\sin\phi \quad (52)$$

$$u_x' = -r\Omega\sin\theta\sin\phi \quad (53)$$

$$u_y' = r\Omega\sin\theta\cos\phi \quad (54)$$

$$T_p' = T_p - ar(\sin\theta\sin\phi). \quad (55)$$

Utilizing the fact that in the dilute limit, the bulk temperature gradient $\langle\partial T/\partial x_i\rangle$ represents only an order v correction over the far field temperature gradient a, the corresponding independent components of the effective conductivities can be found from equation (37). When nondimensionalized by k_f, they are (correct to order v)

$$\frac{K_{xy}}{k_f} = v\left\{\left(\frac{k_p}{k_f}-1\right)\bar{B} - 0.2Pe\frac{k_p}{k_f} + \frac{k_p}{k_f}\left\{\sinh\beta\cos\beta\left(C+\frac{3\bar{C}}{Pe}\right)+\sin\beta\cosh\beta\left(\frac{3C}{Pe}-\bar{C}\right) + \frac{3}{\sqrt{(2Pe)}}[\sin\beta\sinh\beta(\bar{C}-C) - \cos\beta\cosh\beta(C+\bar{C})]\right\}\right. \quad (56)$$

and

$$\frac{K_{yy}}{k_f} = 1+v\left\{\left(\frac{k_p}{k_f}-1\right)(1+B) - \frac{k_p}{k_f}\left\{\sin\beta\cosh\beta\left(C+\frac{3\bar{C}}{Pe}\right)+\sinh\beta\cos\beta\left(\bar{C}-\frac{3C}{Pe}\right) + \frac{3}{\sqrt{(2Pe)}}[\cos\beta\cosh\beta(C-\bar{C}) - \sin\beta\sinh\beta(C+\bar{C})]\right\}\right. \quad (57)$$

where β, B, C and $\bar{C}$ were defined in Section 2. The results for K_{yy} and K_{xy} are plotted in Figs. 5 and 6, respectively.

Figure 5 shows a plot of the transversely isotropic component, K_{yy} as a function of Peclet number for a variety of conductivity ratios k_f/k_p. The results are plotted as $(K_{yy}/k_f-1)/v$ in order to highlight the conductivity augmentation caused by the presence of the rotating particle. At $Pe = 0$ the conductivity enhancement follows Maxwell's [6] predictions for a dispersion of stationary spheres. Increasing the Peclet number increases the effective conductivity until the curves asymptotically approach the limiting value of 3.0, which corresponds to Maxwell's solution in the limit of infinite particle conductivity (i.e. as $k_f/k_p \to 0$). This confirms the prediction from the dimensional analysis that infinite Peclet number is equivalent to infinite particle conductivity. However, the approach to the infinite conductivity limit is surprisingly slow. For example, the $k_f/k_p = 1$ curve—a case that would not be uncommon in suspensions—requires a Peclet number of 1000 or so to get near to the limit; this is much larger than the Peclet numbers found in the experiments of ref. [1]. Furthermore, if the particle already has a large conductivity (small k_f/k_p), the effective conductivity is already pushing against this upper limit, and rotation can only make a small contribution to the heat transport. (Maxwell also pre-

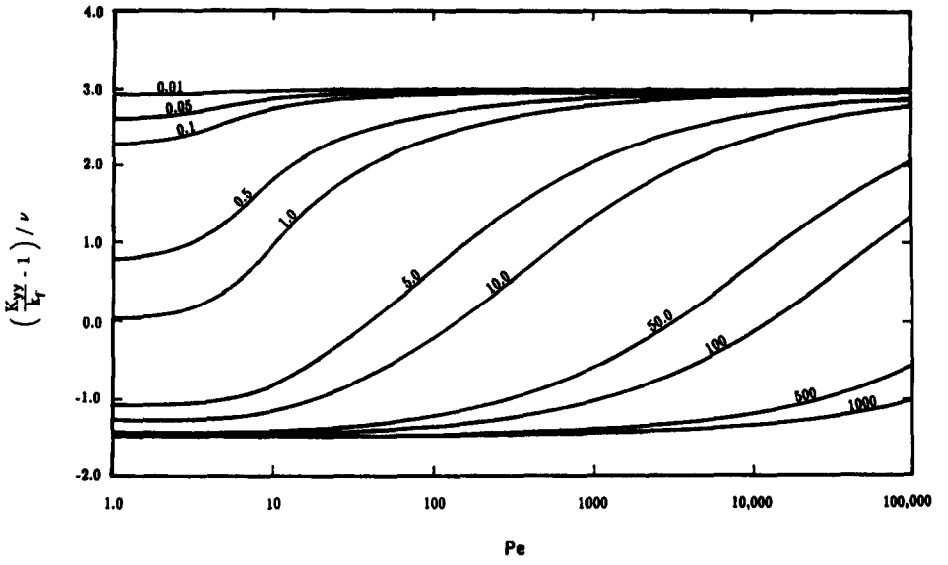

FIG. 5. The transversely isotropic conductivity, K_{yy}, as a function of particle Peclet number. The numbers on the lines are the conductivity ratios k_f/k_p.

dicted that $(K_{yy}/k_f)/\nu \to -1.5$ as $k_f/k_p \to \infty$, which may be clearly seen as the lower limit in Fig. 5.)

Figure 6 shows a plot of the anisotropic component, $K_{xy}/(\nu k_f)$, as a function of Peclet number. As anticipated in the last section, the anisotropy goes to zero as $Pe \to 0$ and as $Pe \to \infty$. This supports the conclusion that as $Pe \to \infty$ the system behaves as if it were composed of non-rotating particles with infinite conductivity; in this limit, the system must obey Maxwell's solution and hence must be isotropic. Furthermore, very little anisotropy is generated with high conductivity particles, reflecting the fact that, in these cases, rotation produces very little change in the external isotherms. The largest magnitude corresponds to $k_f/k_p = 1$ and occurs at $Pe \simeq 10$, for which the isotherms are plotted in Fig. 2(b). For larger values of k_f/k_p, the magnitude of the maximum anisotropy both decreases slightly and is reached at progressively larger and larger values of Pe. Note that the maximum anisotropy for the $k_f/k_p = 10$ curve occurs at $Pe \simeq 500$, the isotherms for which are plotted in Fig. 4(e). This should not be surprising since the external isotherms in Fig. 4(e) were previously noted to be identical to those in Fig. 2(b), which indicates some relationship between this isotherm pattern and the maximum anisotropy.

5. CONCLUSIONS

In interpreting the results of their experiments on the heat transfer to sheared particulate materials,

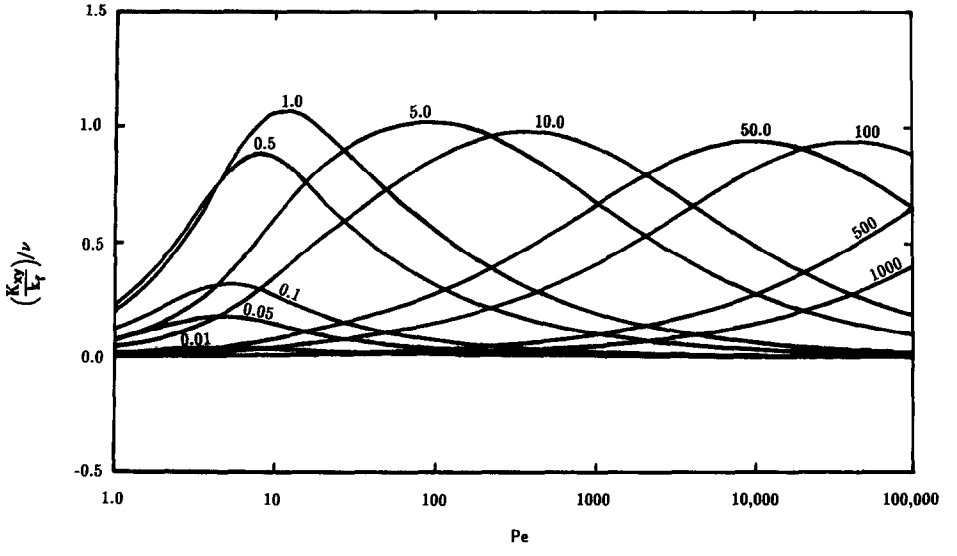

FIG. 6. The anisotropic conductivity, K_{xy}, as a function of the particle Peclet number. The numbers on the lines are the conductivity ratios, k_f/k_p.

Campbell and Wang [1] identified shear-induced particle rotation as one mechanism to explain the mechanical improvement in the effective conductivity of the material. They speculated that a particle rotating in a temperature gradient would absorb heat as the surface passed through the hot portion of the temperature gradient and discharge it while passing through the cold portion. Thus the rotation induces microscale level convection which should make a turbulence-like improvement in the internal heat transport rates.

To gain a fundamental understanding of this mechanism, this paper has analyzed the case of a single particle rotating in an infinite medium on which is imposed a uniform temperature gradient. Much of the important information was immediately gleaned from the dimensionless equations, which indicated that increasing the rotational Peclet number increases the apparent conductivity of the particles and that, in the limit of infinite Peclet number, the composite would behave as if all of the particles had infinite thermal conductivity. A consequence of this observation was that, in the particle–air mixtures used in ref. [1], the conductivity ratio between the dispersed and continuous phases was already so large that particle rotation had little effect. The dimensional argument was validated by examining the isotherm patterns, which also indicated that, at moderate Peclet numbers, the rotation induces thermal anisotropy within the material. The anisotropy could be observed to disappear both at $Pe = 0$ and as $Pe \to \infty$.

The last step was to determine the effective conductivity tensor for the composite material in the dilute limit using a classic volume averaging technique. The results show that the isotropic conductivity increases monotonically with Peclet number and asymptotically approaches the value predicted by Maxwell [3] for a dispersion of stationary particles with infinite conductivity. In addition, the anisotropy of the thermal conductivity grows for low Peclet number, reaches a maximum, and then asymptotically approaches zero as $Pe \to \infty$. Both of these observations could be predicted by examining the pattern of isotherms about the particles, and collectively they support the dimensional arguments which predict that, at large Pe, the particles behave as if they have infinite thermal conductivity.

Acknowledgements—The authors thank Prof. J. D. Godard for his insights on the effective conductivity controversy. This work was supported by the National Science Foundation under Grants MEA 84-04415, MEA 83-52513 and CBT 86-15160. Additional funding was provided by IBM and the Air Force Office of Scientific Research under grant AFOSR 87-0284. The authors are most grateful for this generous support.

REFERENCES

1. C. S. Campbell and D. G. Wang, The effective conductivity of shearing particle flows, *Proc. 8th Int. Heat Transfer Conf.*, Vol. 5, pp. 2567–2572. Hemisphere, Washington, DC (1986).
2. C. S. Campbell, The stress tensor for simple shear flows of a granular material, *J. Fluid Mech.* **203**, 449–473.
3. J. C. Maxwell, *Electricity and Magnetism* (1st Edn). Oxford University Press, London (1873).
4. L. G. Leal, On the effective conductivity of dilute suspension of spherical drops in the limit of low particle Peclet number, *Chem. Engng Commun.* **1**, 21–31 (1973).
5. A. Nir and A. Acrivos, The effective thermal conductivity of sheared suspensions, *J. Fluid Mech.* **78**, 33–48 (1976).
6. Y. C. Chung and L. G. Leal, An experimental study of the effective thermal conductivity of a sheared suspension of rigid spheres, *Int. J. Multiphase Flow* **8**(6), 605–625 (1982).
7. L. G. Leal, Macroscopic transport properties of a sheared suspension, *J. Colloid Interface Sci.* **58**(2), 296–311 (1977).

LA ROTATION D'UNE PARTICULE COMME MECANISME DE TRANSFERT THERMIQUE

Résumé—Une particule qui tourne dans un gradient de température absorbe de la chaleur du côté chaud du gradient et la rejète du côté froid. On examine le cas d'une sphère solide en rotation dans un milieu stationnaire sur lequel on impose un gradient de température uniforme. Les résultats montrent que la rotation augmente le transport d'énergie interne de la même façon que la conductivité thermique de la particule. Pour des valeurs modérées du nombre de Peclet rotationnel, la rotation induit des anisotropies dans la conductivité thermique apparente du matériau qui disparaissent à $Pe = 0$ et aussi à $Pe \to \infty$.

ROTATION EINES PARTIKELS ALS WÄRMEÜBERTRAGUNGSMECHANISMUS

Zusammenfassung—Ein Partikel, das in einem Medium mit aufgeprägtem Temperaturgradienten rotiert, nimmt Wärme an der heißen Seite auf und gibt sie an der kalten Seite wieder ab. Die vorliegende Arbeit befaßt sich mit dem Fall einer rotierenden Kugel in einem ruhenden Medium bei konstantem Temperaturgradienten. Die Ergebnisse zeigen, daß die Rotation den Wärmetransport im Medium umso stärker vergrößert, je höher die Wärmeleitfähigkeit des Partikels ist. Bei mittleren Werten der Rotations-Peclet-Zahl ergibt sich eine Anisotropie der effektiven Wärmeleitfähigkeit des Mediums, welche für $Pe = 0$ und $Pe \to \infty$ verschwindet.

ВРАЩЕНИЕ ЧАСТИЦЫ КАК МЕХАНИЗМ ТЕПЛОПЕРЕНОСА

Аннотация—В среде с температурным градиентом вращающаяся частица поглощает тепло от нагретой части и отдает его холодной. Рассматривается случай твердой сферы, вращающейся в стационарной среде с однородным температурным градиентом. Результаты показывают, что вращение частицы таким же образом влияет на улучшение переноса внутренней энергии, как и увеличение коэффициента теплопроводности частицы. При средних значениях вращательного числа Пекле вращение вызывает анизотропию кажущегося коэффициента теплопроводности материала, исчезающей при $Pe = 0$ и $Pe \to \infty$.